Astronomy & Astrophysics manuscript no. c5s˙irc
August 28, 2014
© ESO 2014

arXiv:1408.6306v1 [astro-ph.GA] 27 Aug 2014

New molecules in IRC +10216: confirmation of C_5S and tentative identification of MgCCH, NCCP, and SiH_3CN⋆

Marcelino Agúndez[1], José Cernicharo[1], and Michel Guélin[2]

[1] Instituto de Ciencia de Materiales de Madrid, CSIC, C/ Sor Juana Inés de la Cruz 3, 28049 Cantoblanco, Spain
[2] Institut de Radioastronomie Millimétrique, 300 rue de la Piscine, 38406 St. Martin d'Héres, France

Received; accepted

ABSTRACT

The C-star envelope IRC +10216 harbors a rich variety of molecules, with more than 80 detected to date. During the course of a λ 3 mm survey of IRC +10216 carried out with the IRAM 30-m telescope we have detected various weak lines, with antenna temperatures of a few mK, that we assign to rotational transitions of four new molecules. The observation of three lines of C_5S confirms a previous tentative identification of this molecule by Bell et al. (1993) based on a line at 24.0 GHz. We also report the tentative identification of three molecules not yet observed in space: MgCCH, the first metal acetylide detected in space, and NCCP and SiH_3CN, the phosphorus and silicon analogs of cyanogen (NCCN) and methyl cyanide (CH_3CN). We derive the following column densities: $N(C_5S) = (2\text{-}14) \times 10^{12}$ cm^{-2} (depending on the rotational temperature adopted), $N(\mathrm{MgCCH}) = 2 \times 10^{12}$ cm^{-2}, $N(\mathrm{NCCP}) = 7 \times 10^{11}$ cm^{-2}, and $N(SiH_3CN) = 10^{12}$ cm^{-2}. The S-bearing carbon chain C_5S is less abundant than C_3S, while MgCCH has an abundance in between that of MgNC and those of MgCN and HMgNC. On the other hand, NCCP and SiH_3CN are the least abundant P- and Si-bearing molecules observed to date in IRC +10216. Based on the behavior of similar molecules it is likely that these four species are formed in the outer circumstellar layers of IRC +10216. We discuss possible gas-phase formation routes.

Key words. astrochemistry – stars: circumstellar matter – stars: AGB and post-AGB – stars: carbon – stars: individual: IRC +10216 – radio lines: stars

1. Introduction

The C-star envelope IRC +10216 is one of the richest molecular sources in the sky, with more than 80 molecules discovered to date. The central star being at the tip of the AGB phase, it is expelling matter at a high rate of $\sim 2 \times 10^{-5}$ M$_\odot$ yr^{-1}, and being relatively nearby (~130 pc), it is the prototype of carbon star. The inner wind is a factory of dust and relatively stable molecules while in its outer layers the photochemistry driven by the penetration of interstellar UV photons produces a wealth of exotic molecules.

IRC +10216 has been intensively observed from cm- to submm-wavelengths, including various line surveys (see a review in Cernicharo et al. 2011). Because of the carbon-rich character of the star, the molecular inventory of the envelope is dominated by carbon chains such as polyyne and cyanopolyyne radicals (Cernicharo & Guélin 1996; Guélin et al. 1998), carbon chains containing sulfur or silicon (Cernicharo et al. 1987; Ohishi et al. 1989; Bell et al. 1993), exotic molecules containing phosphorus or metals (Halfen et al. 2008; Cabezas et al. 2013), and negatively charged carbon chains (McCarthy et al. 2006; Cernicharo et al. 2007; Agúndez et al. 2010).

During the last decades IRC +10216 has been widely observed with the IRAM 30-m telescope, covering most of the atmospheric spectral windows available at wavelengths of 3, 2, 1.3, and 0.9 mm. In particular, the line survey in the 3 mm band has reached a very high sensitivity in certain spectral regions, allowing to detect very weak features at the level of a few mK of antenna temperature. Here we report various weak lines observed within the λ 3 mm band, three of which are assigned to C_5S, confirming a previous tentative identification of this molecule based on a line at cm-wavelengths (Bell et al. 1993), while others are tentatively attributed to the molecules MgCCH, NCCP, and SiH_3CN.

2. Observations

The observations were made with the IRAM 30-m telescope located at Pico Veleta (Spain) during several sessions, most of them between 2002 and 2008 in the context of a λ 3 mm line survey of IRC +10216 covering the frequency range 80-116 GHz. The full 3 mm line survey will be published soon elsewhere. The old ABCD receivers, currently replaced by EMIR at the 30m telescope, were used. A SIS receiver operating at 3 mm was tuned in single sideband mode, with a typical image rejection larger than 20 dB. Identification of image side band lines was done by shifting the frequency of the local oscillator. Data were taken in the wobbler switching observing mode by nutating the secondary mirror by 3-4′ at a rate of 0.5 Hz. Pointing and focus were checked by observing nearby planets and the quasar OJ 287. The back end used was a filterbank with a bandwidth of 512 MHz and a spectral resolution of 1.0 MHz. The intensity scale was calibrated using two absorbers at different temperatures and the atmospheric transmission model ATM (Cernicharo 1985; Pardo et al. 2001). We express intensities in terms of T_A^*, the antenna temperature corrected for atmospheric absorption and for antenna ohmic and spillover losses. The uncertainty in T_A^* due to calibration is estimated to be around 10 %. The system temperature ranged from 100 to 150 K. On source integra-

⋆ Based on observations carried out with the IRAM 30m Telescope. IRAM is supported by INSU/CNRS (France), MPG (Germany) and IGN (Spain).

Table 1. Line parameters observed in IRC +10216

Transition	ν_{calc} (MHz)	ν_{obs} (MHz)	V_{exp} (km/s)	$\int T_A^* dv$ (K km/s)
$J' - J''$		C_5S		
44-43	81192.98	81193.4(10)[a]	14.5[b]	0.09(3)
45-44	83038.05	83037.8(4)	13.7(8)	0.05(1)
46-45	84883.09	84883.5(10)	16.3(20)	0.08(2)
$N'_{J'} - N''_{J''}$		MgCCH		
$9_{17/2}$-$8_{15/2}$	89361.27	89361.0(15)	14.5[b]	0.03(1)
$9_{19/2}$-$8_{17/2}$	89377.76	89378.0(15)	14.5[b]	0.03(1)
$10_{19/2}$-$9_{17/2}$	99289.52	99288.5(10)	14.5[b]	0.04(1)
$10_{21/2}$-$9_{19/2}$	99306.01	99305.6(10)	14.5[b]	0.07(2)
$J' - J''$		NCCP		
15-14	81131.69	81131.9(10)	14.5[b]	0.03(1)
16-15	86540.07	86539.5(10)	14.5[b]	0.05(1)
18-17	97356.60	97355.7(10)	12.4(15)	0.06(2)
$J'_{K'} - J''_{K''}$		SiH_3CN[c]		
9_0-8_0	89509.90	89509.5(10)	16.7(15)	0.05(1)
9_1-8_1	89508.76			
10_0-9_0	99454.36	99452.5(15)[a]	14.7(15)	0.08(2)
10_1-9_1	99453.08			
11_0-10_0	109398.46	109397.0(15)[a]	14.5[b]	0.09(3)
11_1-10_1	109397.06			

Numbers in parentheses are 1σ uncertainties in units of the last digits. [a] Line blended. [b] Line width has been fixed. [c] The K=0,1 components of SiH_3CN (the strongest ones) are fit to one single line.

tion times ranged from 2 to 20 hours, resulting in T_A^* rms noise levels per 1 MHz channel ranging from less than 1 mK to 3 mK.

3. Results and discussion

3.1. C_5S

The molecule C_5S is a relatively heavy linear carbon chain with a $^1\Sigma^+$ ground electronic state, whose rotational spectrum has been recorded in the laboratory in the 5-18 GHz frequency range (Kasai et al. 1993; Gordon et al. 2001). Its electric dipole moment has been calculated as 4.65 D (Pascoli & Lavendy 1998; Pérez-Juste et al. 2004). In their observations of IRC +10216 using the NRAO 140-foot radiotelescope, Bell et al. (1993) reported the detection of a line at 23990.2 MHz which was tentatively assigned to the $J = 13 - 12$ rotational transition of C_5S. To our knowledge, this tentative detection has not been neither confirmed nor refuted by subsequent studies.

Various rotational transitions of C_5S with upper level energies E_{up} in the range 90-170 K fall within the frequency coverage of our 3 mm line survey. We have identified at the lower frequency side of the survey three weak emission lines whose frequencies coincide with the $J = 44-43$ to $J = 46-45$ transitions of C_5S. The next J lines are not detected either because they fall in spectral regions observed with an insufficient sensitivity or because they overlap with other strong lines (see Appendix A). The line parameters are given in Table 1 and the lines are shown in Fig. 1. The agreement between calculated and observed frequencies is better than 1 MHz, which is good enough taking into account the moderate spectral resolution of the observed spectra (1 MHz) and the non-negligible errors of some hundreds of kHz in the calculated frequencies at 3 mm (extrapolated from laboratory measurements at cm-wavelengths). In IRC +10216's spectra the $J = 45 - 44$ and $J = 46 - 45$ lines of C_5S appear free of blending with other lines, although the $J = 44 - 43$ line overlaps partially with other weak lines arising from $HC^{13}C^{13}CN$ and $CCCC^{13}CH$.

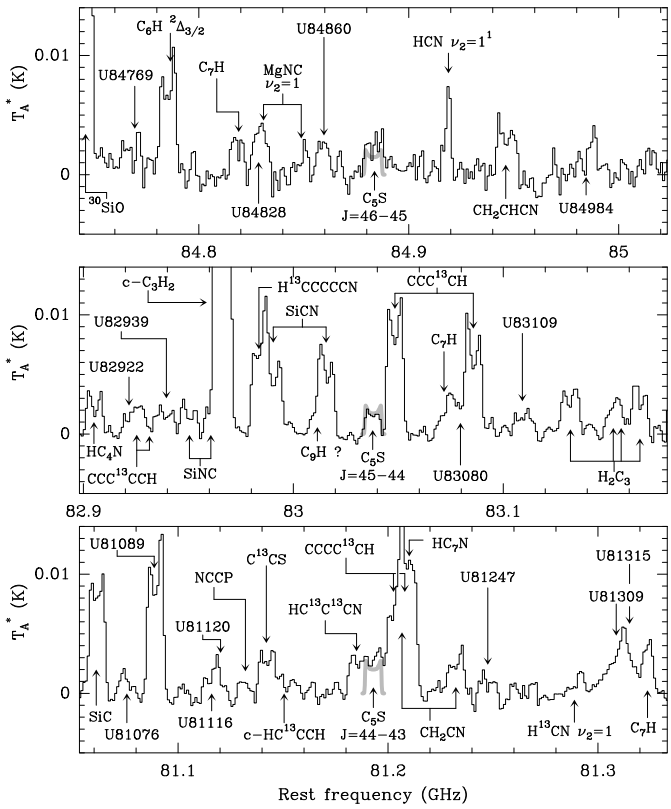

Fig. 1. Portions of the 3 mm line survey of IRC +10216 showing the $J = 44 - 43$, $J = 45 - 44$, and $J = 46 - 45$ lines of C_5S. The $J = 44 - 43$ line is blended with lines of $HC^{13}C^{13}CN$ and $CCCC^{13}CH$. The T_A^* rms noise levels per 1 MHz channel are 0.6, 0.5, and 1.0 mK in the bottom, middle, and top panels, respectively. Note the coincidence in frequency of a weak shoulder at the red part of a SiCN line with the $^2\Pi_{3/2}$ $J = 201/2 - 199/2$ line of C_9H (middle panel). Thick gray lines are the calculated line profiles under LTE assuming that C_5S extends between 5 and 20″ with an homogeneous fractional abundance and rotational temperature of 18 K.

Given the limited signal-to-noise ratio of the C_5S lines it is difficult to appreciate a distinct line shape, either U-shaped or flat-topped, which could permit us to infer whether the size of the emitting region is smaller or larger than the main beam of the telescope at these frequencies (29-30″). Based on the U-shaped line profiles observed at 3 mm for the related molecules C_2S and C_3S (Cernicharo et al. 1987) we could also expect an extended emission for C_5S. Assuming a source size of radius 20″, as most molecules distributed as a hollow shell in IRC +10216 (e.g., Guélin et al. 1997), and adopting the intensities of the three lines observed at 3 mm and that observed by Bell et al. (1993) at 24.0 GHz, we derive a column density $N(C_5S)$ of 1.4×10^{13} cm^{-2} and a rotational temperature T_{rot} of 18 K. The column density is somewhat lower than that reported by Bell et al. (1993), mainly because of the lower source size adopted by these authors. The derived values of T_{rot} and $N(C_5S)$ rely to a large extent on the 0.8 cm line (E_{up} = 8 K) observed by Bell et al. (1993). If we only consider the lines at 3 mm (E_{up} = 88-96 K) then T_{rot} needs to be fixed and $N(C_5S)$ becomes very sensitive to the adopted choice of T_{rot}. For example, for a rotational temperature of 44 K (as measured for the related molecule C_3S; see Table 2) the column density of C_5S decreases by almost one order of magnitude to 2×10^{12} cm^{-2}. The 3 mm lines involve high energy

Table 2. Rotational temperatures and column densities

Molecule	T_{rot} (K)	N (cm^{-2})	Reference
C_2S	18(1)	$5.0(3) \times 10^{13}$	[1]
C_3S	44(2)	$1.7(1) \times 10^{13}$	[1]
C_4S	20 [a]	$<7 \times 10^{12}$ [b]	[2]
C_5S	18-44	$(2\text{-}14) \times 10^{12}$	[2]
MgCCH	20 [a]	2×10^{12}	[2]
NCCP	20 [a]	7×10^{11}	[2]
SiH_3CN	39 [a]	1×10^{12}	[2]

Numbers in parentheses are 1σ uncertainties in units of the last digits. A source size of radius 20″ has been adopted. [a] T_{rot} has been fixed. [b] 3σ upper limit.
References: [1] IRAM 30-m data at λ 3, 2, and 1.3 mm. [2] This study.

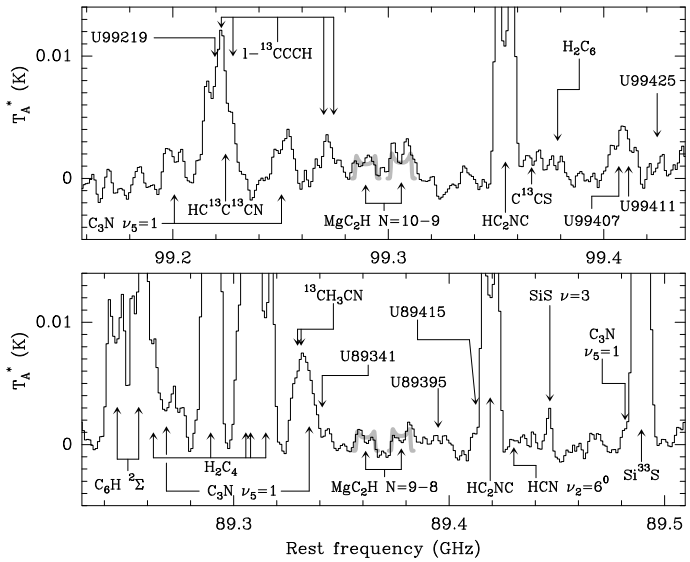

Fig. 2. Parts of the 3 mm line survey of IRC +10216 showing the couples of lines tentatively assigned to the $N = 9 - 8$ and $N = 10 - 9$ doublets of MgCCH. The T_A^* rms noise levels per 1 MHz channel are 0.5 and 0.7 mK in the bottom and top panels, respectively. Thick gray lines correspond to the calculated line profiles under LTE assuming that MgCCH extends between 5 and 20″ with an homogeneous fractional abundance and rotational temperature of 20 K.

levels and have Einstein coefficients for spontaneous emission (and thus critical densities) about 40 times higher than the 0.8 cm line, probably implying that they are subthermally excited in the outer layers of IRC +10216 and that C_5S is not characterized by a uniform rotational temperature. For T_{rot} = 18-44 K we find that C_5S has a column density in the range (2-14) $\times 10^{12}$ cm^{-2}. Fig. 1 shows the line profiles calculated under local thermodynamic equilibrium (LTE) adopting the parameters of the envelope from Agúndez et al. (2012) and assuming that C_5S is present in a hollow shell extending from 5 to 20″, with an homogeneous fractional abundance and rotational temperature of 18 K, which may be adequate for the 3 mm lines, as discussed above. The agreement between modeled and observed line profiles is fairly good.

The molecule C_5S is the largest member of the series of sulfur-containing carbon chains C_nS observed in space. The shorter members C_2S and C_3S are observed in various astronomical regions, although C_4S has never been observed. The column densities derived for these molecules in IRC +10216 are given in Table 2. In the cases of C_2S and C_3S the column densities are quite robust as they result from a large number of rotational lines observed across the 3, 2, and 1.3 mm bands. That of C_4S is just an upper limit while that of C_5S has a large uncertainty, which however could be reduced if sensitive observations are performed at frequencies around 40 GHz, where the brightest C_5S lines are expected. This spectral region has been surveyed by Kawaguchi et al. (1995) although no line attributable to C_5S was found, probably due to an insufficient sensitivity. The carbon chains C_nS seem to show a decline in abundance as the length of the chain increases (albeit the uncertainty in the value of C_5S), as occurs with polyacetylenic and cyanopolyacetilenic chains (see e.g. Agúndez et al. 2008a). There is no obvious alternation in the abundance between chains with n odd ($^1\Sigma$ electronic ground state) and those with an even number of carbon atoms ($^3\Sigma$ electronic ground state), as may be occurring for the series C_nO, of which only C_3O, but not C_2O, has been detected in IRC +10216 (Tenenbaum et al. 2006). It is also worth noting that the rotational temperature of C_3S is more than twice that of C_2S (see Table 2), which points to differences in the excitation and may be indicative of radiative pumping to vibrationally excited states playing an important role in the case of C_3S (see e.g., Agúndez et al. 2008a).

The chemical routes leading to S-bearing carbon chains in IRC +10216 have been investigated by Millar et al. (2001), who find that the synthesis is probably dominated by reactions of the type

$$S + C_{2n}H \rightarrow C_{2n}S + H, \qquad n = 1, 2, ... \tag{1}$$

for S-containing carbon chains with an even number of carbon atoms, while those with an odd number of carbon atoms would form through reactions of the type

$$CS + C_{2n}H \rightarrow C_{2n+1}S + H, \qquad n = 1, 2, ... \tag{2}$$

The model of Millar et al. (2001) yields results in reasonable agreement with our observed column densities of C_nS chains, although these are somewhat overestimated by the model probably because of the too high initial abundance of CS adopted (4 $\times 10^{-6}$ relative to H_2), which may need to be revised down by a factor of 5-6 (Agúndez et al. 2012).

3.2. MgCCH

A variety of metal cyanides has been observed in the circumstellar gas of IRC +10216, among them various involving magnesium such as the isocyanic and cyanic forms MgNC and MgCN (Guélin et al. 1986; Kawaguchi et al. 1993; Ziurys et al. 1995), and more recently the hydrogenated isocyanic form HMgNC (Cabezas et al. 2013). Metals thus show a tendency to combine with cyanide radicals rather than other types of radicals in IRC +10216. The ethynyl radical being as abundant as the cyanide radical in IRC +10216 it is therefore reasonable to expect that metal acetylides such as MgCCH could also be present in the circumstellar gas. Magnesium monoacetylide (MgCCH) is a linear radical with a $^2\Sigma^+$ electronic ground state, whose pure rotational spectrum has been characterized in the laboratory in the spectral range 315-525 GHz (Brewster et al. 1999). MgCCH has a moderate electric dipole moment of 1.68 D, according to the ab initio calculations of Woon (1996), which indicates that the ethynyl-metal bond probably has a fair degree of covalent character.

Three rotational transition doublets of MgCCH fall within our 3 mm line survey. The $N = 9 - 8$ and $N = 10 - 9$ at 89.3

and 99.3 GHz, respectively, coincide in frequency with two pairs of non-blended weak lines (see Fig. 2) while the $N = 11 - 10$ at 109.2 GHz falls in a region where the sensitivity of the spectrum is insufficient to detect lines with antenna temperatures of a few mK (see Appendix A). The agreement between observed and calculated frequencies is reasonably good, less than 1 MHz (see Table 1). It must however be taken into account that the observed lines attributed to MgCCH are weak and the number of lines with similar intensities is relatively large in this region of the spectrum and at this level of sensitivity. The possibility of accidental coincidence cannot be completely ruled out although the assignment to MgCCH is reinforced by the fact that the transitions consist of doublets and both the $N = 9-8$ and $N = 10-9$ are observed free of blending. Nonetheless, for the moment we prefer to rest cautious and consider the detection of MgCCH as tentative, mainly because of the weakness of the observed lines.

Despite the limited signal-to-noise ratio of the MgCCH lines observed, these seem to show a U-shaped profile, which would indicate that the size of the emission is comparable or larger than the main beam of the IRAM 30-m telescope at the observed frequencies (25-28″). Magnesium isocyanide has been found to be distributed in the form of a hollow shell of radius 15-20″, as mapped with the IRAM Plateau de Bure interferometer at millimeter wavelengths (Guélin et al. 1993). Based on the U-shaped profiles and the distribution of the related molecule MgNC we can assume a source size of radius 20″ for MgCCH. Adopting a rotational temperature of 20 K, of the order of other molecules distributed in the outer layers of IRC +10216 (Cernicharo et al. 2000), we derive a column density N(MgCCH) of 2×10^{12} cm^{-2}, that is, ∼6 times less than MgNC and ∼3 times above those of MgCN and HMgNC (Cabezas et al. 2013). As shown in Fig 2, the MgCCH line profiles calculated under LTE assuming a rotational temperature of 20 K are in reasonable agreement with the observations.

The possible chemical routes leading to metal-containing molecules, including MgCCH, in the outer layers of IRC +10216 have been addressed in various studies (Woon 1996; Petrie 1996; Dunbar & Petrie 2002; Millar 2008). Various chemical pathways have been ruled out based on reaction endothermicities or on the lack of sufficiently abundant precursors in the circumstellar gas. From these studies it turns out that the most likely formation route of MgCCH probably follows closely that proposed by Petrie (1996) for the synthesis of magnesium cyanides, which consists of the radiative association between Mg^+ and large cyanopolyynes followed by the dissociative recombination of the ionic complex with free electrons. In the case of MgCCH, the radiative recombination would take place between Mg^+ and large polyynes, leading to $Mg(C_nH_2)^+$ complexes, whose recombination with electrons could yield MgCCH, among other possible fragments. A simple chemical model similar to that described in Cabezas et al. (2013) adopting the rate constants of radiative association between Mg^+ and polyynes calculated by Dunbar & Petrie (2002) indicates that this route is capable of producing MgCCH with an abundance high enough to account for the column density derived from observations. An alternative route could be the exchange reaction between MgNC and CCH to yield MgCCH and CN (the precursor MgNC being about 6 times more abundant than MgCCH in IRC +10216), although theoretical calculations do not conclude whether this reaction is slightly endothermic or slightly exothermic (Woon 1996). Other metal acetylides could be present in IRC +10216, although they may be difficult to detect if, as found in the case of Mg, they are less abundant than the corresponding (iso)cyanides. For example, AlNC is detected in IRC +10216 (Ziurys et al. 2002) but not

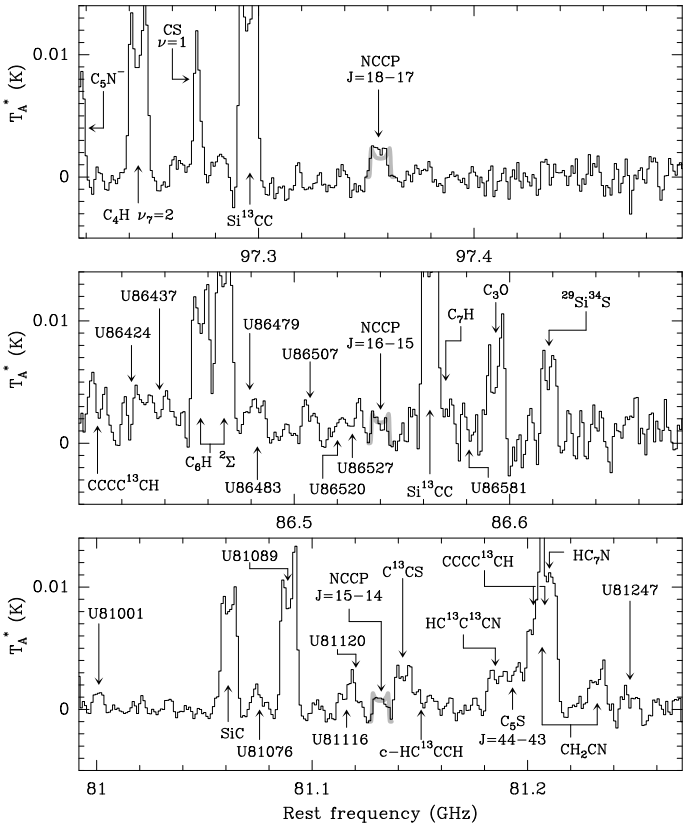

Fig. 3. Parts of the 3 mm line survey of IRC +10216 showing the three lines tentatively assigned to the $J = 15 - 14$, $J = 16 - 15$, and $J = 18-17$ rotational lines of NCCP. The $J = 16-15$ line is marginally detected. The T_A^* rms noise levels per 1 MHz channel are 0.4, 1.2, and 0.8 mK in the bottom, middle, and top panels, respectively. Line profiles calculated under LTE assuming that NCCP extends between 5 and 20″ with an homogeneous fractional abundance and rotational temperature of 20 K are shown as thick gray lines.

AlCCH, with N(AlCCH)/N(AlNC) $\lesssim 22$ (Cabezas et al. 2012). The low dipole moment of AlCCH (∼0.6 D) makes it difficult to impose a stringent upper limit on its abundance.

3.3. NCCP

From a chemical point of view, cyanophosphaethyne (NCCP) can be viewed as a cyanogen molecule (NCCN) in which a nitrogen atom has been substituted by a phosphorus atom. From a spectroscopic point of view, NCCP is a linear molecule with a closed-shell singlet electronic ground state. Its pure rotational spectrum has been characterized in the laboratory over a broad spectral range, from 25 to 820 GHz (Bizzocchi et al. 2001). Having a moderately large dipole moment of 3.44 D, as measured by Cooper et al. (1980), it has been suggested that this molecule could be a good candidate for detection in astronomical sources such as IRC +10216 (Bizzocchi et al. 2001), where other P-bearing molecules such as CP, PN, HCP, PH_3, and CCP have been already detected (Guélin et al. 1990, 2000; Agúndez et al., 2007, 2008b, 2014; Milam et al. 2008; Tenenbaum & Ziurys 2008; Halfen et al. 2008).

Seven rotational lines of NCCP from $J = 15 - 14$ to $J = 21 - 20$, with upper level energies in the range 30-60 K, fall within the 3 mm line survey. A weak line with T_A^* ∼2-3 mK ly-

ing at 97355.7 ± 1 MHz coincides in frequency, within less than 1 MHz, with the $J = 18-17$ transition of NCCP (see Table 1 and Fig. 3). To confirm whether this assignment is correct we have searched for other rotational transitions of NCCP within the 3 mm band. A weak line at 81131.9 ± 1 MHz, lying in one of the most sensitive regions of the 3 mm spectrum, might be assigned to the $J = 15 - 14$ transition while the $J = 16 - 15$ can be identified with a marginal line at 86539.5 ± 1 MHz. The rest of transitions of NCCP within the 3 mm band either fall in regions where the sensitivity achieved is insufficient to detect such weak lines or are affected by severe blendings with other strong lines (see Appendix A). The agreement between calculated and observed frequencies is reasonably good and, within the sensitivity reached, there are not missing lines in the 3 mm line survey. On the other hand, line confusion and accidental coincidence may be an issue at this level of sensitivity in the 3 mm spectra of IRC +10216. We must therefore be cautious and consider the identification of NCCP as tentative.

Given the limited signal-to-noise ratio of the three lines assigned to NCCP it is difficult to distinguish whether the line profiles are more U-shaped or flat-topped. Assuming that this molecule is formed in the outer layers, as seems to be the case of the related radical CCP (Halfen et al. 2008), we may adopt for NCCP a distribution size with a radius of 20″ and a rotational temperature of 20 K, typical parameters for molecules distributed in the outer shells. The column density of NCCP derived is then 7×10^{11} cm^{-2}, about 50-100 times less abundant than CP and slightly less abundant than CCP. The column densities of CP and CCP in IRC +10216 are in the ranges 3.9-8 $\times 10^{13}$ and 1.2-2.9 $\times 10^{12}$ cm^{-2}, respectively, according to Guélin et al. (1990), Halfen et al. (2008), and an analysis of our IRAM 30-m data. As can be seen in Fig 3, the line profiles of NCCP calculated under LTE assuming a rotational temperature of 20 K show a good agreement with the observed ones.

The chemistry of phosphorus-containing molecules in circumstellar envelopes such as IRC +10216 has been discussed by MacKay & Charnley (2001) and Agúndez et al. (2007), although the formation of NCCP has not yet been addressed. Little is known on the chemical kinetics of this species. We can imagine that formation routes similar to those yielding cyanogen (NCCN), which are better studied, could also work for NCCP. The formation of NCCN in the reaction of HCN and CN does not occur at low temperatures because of an activation barrier (Yang et al. 1992), although the reaction between HNC and CN may provide an efficient formation route to NCCN as long as the reaction is barrierless and both HNC and CN are abundant in IRC +10216 (Petrie et al. 2003). Unfortunately, NCCN does not have permanent dipole moment and cannot be detected through its rotational spectrum. By analogy with NCCN, we can imagine that NCCP might be efficiently formed in IRC +10216 through the reaction

$$\mathrm{HNC + CP \rightarrow NCCP + H}, \quad (3)$$

which is slightly exothermic, by ∼15 kcal mol^{-1} adopting the formation enthalpy of NCCP from Pham-Tran et al. (2001), and whose reactants are abundant enough in IRC +10216.

3.4. SiH_3CN

Silyl cyanide, SiH_3CN, is a prolate rotor with a closed electronic shell. Its rotational spectrum has been recorded in the laboratory at microwave and millimeter wavelengths and its electric dipole moment has been experimentally determined to be as large as 3.44 D (Priem et al. 1998).

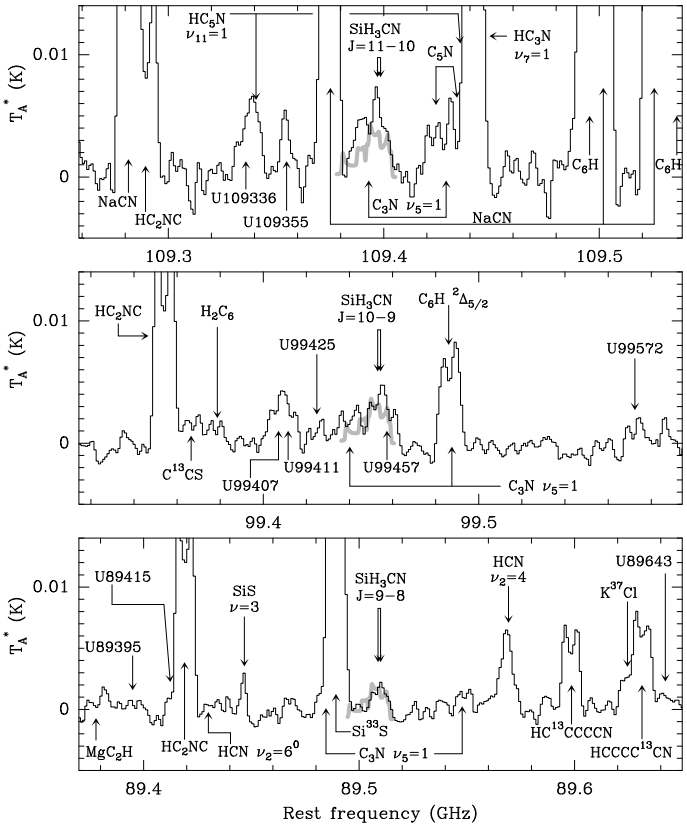

Fig. 4. Portions of the 3 mm line survey of IRC +10216 showing the $J = 9 - 8$ to $J = 11 - 10$ rotational lines of SiH_3CN. Each J line is composed of a set of K components whose line profiles overlap. The $K = 0$ and 1 components, being the strongest, are indicated by arrows. The T_A^* rms noise levels per 1 MHz channel are 0.5, 0.6, and 1.2 mK in the bottom, middle, and top panels, respectively. The $J = 10 - 9$ line is blended with a weak unidentified line at the blue side and both the $J = 10-9$ and $J = 11-10$ lines are blended at the red side with a weak component of C_5N in its $\nu_5 = 1$ vibrational state. These blended lines cannot by themselves explain the whole emission features centered at the frequencies of SiH_3CN. Thick gray lines correspond to the calculated line profiles under LTE assuming that SiH_3CN extends between 5 and 20″ with an homogeneous fractional abundance and rotational temperature of 39 K.

Three rotational transitions of SiH_3CN fall within the 3 mm line survey, $J = 9 - 8$ to $J = 11 - 10$, and the three can be identified with weak emission features in the observed spectrum. Because lines are relatively broad in IRC +10216, ∼29 km s^{-1} or ∼10 MHz at 3 mm, each transition of SiH_3CN is expected to show a complex profile resulting from the overlap of the different K components, the $K = 0$ and 1 being the strongest ones. Fig. 4 shows the SiH_3CN lines while Table 1 gives the line parameters. Only the positions of the $K = 0$ and 1 components are indicated. The $J = 9 - 8$ line appears free of blend with other lines, although the $J = 10 - 9$ and $J = 11 - 10$ overlap partially at the red side with a weak line of C_5N in its $\nu_5 = 1$ vibrational state. Moreover, in the case of the $J = 10 - 9$ line the emission feature observed implies that there must be a weak overlapping unidentified line at ∼99457 MHz. The computation of the line profiles expected for SiH_3CN helps to bring some light into the interpretation of the observed emission features. Assuming that SiH_3CN is distributed as a hollow shell of radius between 5 and

20″ with an homogeneous rotational temperature of 39 K, that derived for the related molecule CH_3CN according to our IRAM 30-m data, a LTE excitation calculation yields the line profiles shown in Fig. 4. It is seen that the line profiles of SiH_3CN are dominated by the $K = 0$ and 1 components with minor contributions from higher K components at lower frequencies. The observed emission features cannot be fully explained by the C_5N $v_5 = 1$ lines and the unidentified line at 99457 MHz, and thus are consistent with the presence of SiH_3CN. However, because two of the three observed transitions of SiH_3CN are partially blended with other lines and because of the limited signal-to-noise ratio achieved, for the moment we consider the identification of SiH_3CN in IRC +10216 as tentative.

A relatively low column density of 10^{12} cm^{-2} is derived for SiH_3CN adopting a rotational temperature of 39 K and a source size of radius 20″, which makes SiH_3CN the least abundant Si-containing molecule detected to date in IRC +10216. Its column density is comparable to, although somewhat below, that of SiCN and SiNC ($\sim 2 \times 10^{12}$ cm^{-2}; Guélin et al. 2000, 2004). The synthesis of SiH_3CN is quite uncertain, although the analogous species CH_3CN has been better studied. A quite direct synthetic pathway to CH_3CN would be the reaction between CH_4 and CN although it has an activation barrier and thus becomes too slow at low temperatures (Sims et al. 1993). In the absence of better constraints we could expect that the route to SiH_3CN from SiH_4 and CN is also probably closed at low temperatures. A more efficient route to CH_3CN in IRC +10216 involves the ion CH_3CNH^+, whose dissociative recombination with electrons yields both CH_3CN and CH_2CN (Agúndez et al. 2008a). In the case of SiH_3CN, a similar route involving the ion SiH_3CNH^+ could also work, although the details on the chemical kinetics of the reactions involved are yet to be investigated.

4. Summary

We have detected various weak lines in the course of a IRAM 30-m λ 3 mm line survey of IRC +10216, three of which are identified with rotational transitions of C_5S, confirming a previous tentative detection of this molecule by Bell et al. (1993) based on a line at 0.8 cm, while some others are tentatively assigned to rotational transitions of three new molecules not yet observed in space. These three molecules are MgCCH, the first metal acetylide detected in space, and NCCP and SiH_3CN, two exotic molecules which are the phosphorus and silicon analogs of cyanogen (NCCN) and methyl cyanide (CH_3CN).

The S-bearing carbon chain C_5S is likely to have a non uniform rotational temperature, with values in the range 18-44 K, which translates to column densities in the range (2-14) $\times 10^{12}$ cm^{-2}, implying that C_5S is less abundant than C_3S in the envelope of IRC +10216. For MgCCH, NCCP, and SiH_3CN we derive column densities of the order of 10^{12} cm^{-2}, which implies that MgCCH has an abundance in between that of MgNC and those of MgCN and HMgNC, while NCCP and SiH_3CN become the least abundant P- and Si-bearing molecules observed to date in IRC +10216.

Based on the behavior of similar molecules it is likely that the four molecules are formed in the outer circumstellar layers of IRC +10216. The synthesis of C_5S probably occurs in a similar fashion to other sulfur-containing carbon chains such as C_3S, while that of MgCCH probably takes place through chemical routes similar to those proposed for the formation of metal cyanides. The formation of NCCP and SiH_3CN is more uncertain and is suggested to occur through analogous pathways to those leading to NCCN and CH_3CN.

The identification of these four molecules through such weak lines suggests that pushing observations towards very low noise levels will probably bring a good number of molecular discoveries in chemically rich environments such as IRC +10216.

Acknowledgements. M.A. and J.C. thank Spanish MINECO for funding support through grants CSD2009-00038, AYA2009-07304, and AYA2012-32032. We thank the anonymous referee for a critical and constructive report.

References

Agúndez, M., Cernicharo, J., & Guélin, M. 2007, ApJ, 662, L91
Agúndez, M., Fonfría, J. P., Cernicharo, J., et al. 2008a, A&A, 479, 493
Agúndez, M., Cernicharo, J., Pardo, J. R., et al. 2008b, A&A, 485, L33
Agúndez, M., Cernicharo, J., Guélin, M., et al. 2010, A&A, 517, L2
Agúndez, M., Fonfría, J. P., Cernicharo, J., et al. 2012, A&A, 543, A48
Agúndez, M., Cernicharo, J., Decin, L., et al. 2014, ApJ, 790, L27
Bell, M. B., Avery, L. W., & Feldman, P. A. 1993, ApJ, 417, L37
Bizzocchi, L., Thornwirth, S., Müller, H. S. P. et al. 2001, J. Mol. Spec., 205, 110
Brewster, M. A., Apponi, A. J., Xin, J. & Ziurys, L. M. 1999, Chem. Phys. Lett., 310, 411
Cabezas, C., Mata, S., Daly, A. M., et al. 2012, J. Mol. Spec., 278, 31
Cabezas, C., Cernicharo, J., Alonso, J. L., et al. 2013, ApJ, 775, 133
Cernicharo, J. 1985, IRAM Internal Report 52
Cernicharo, J., Guélin, M., Hein, H., & Kahane, C. 1987, A&A, 181, L9
Cernicharo, J. & Guélin, M. 1996, A&A, 309, L27
Cernicharo, J., Guélin, M., & Kahane, C. 2000, A&AS, 142, 181
Cernicharo, J., Guélin, M., Agúndez, M., et al. 2007, A&A, 467, L37
Cernicharo, J., Agúndez, M., & Guélin, M. 2011, in The Molecular Universe, ed. J. Cernicharo & R. Bachiller (Cambridge Univ. Press), IAU Symp. 280, 237
Cooper, T. A., Kroto, H. W., Nixon, J. F., & Ohashi, O. 1980, J. Chem. Soc. Chem. Commun., 8, 333
Dunbar, R. C. & Petrie, S. 2002, ApJ, 564, 792
Gordon, V. D., McCarthy, M. C., Apponi, A. J., & Thaddeus, P. 2001, ApJS, 134, 311
Guélin, M., Gómez-González, J., Cernicharo, J., & Kahane, C. 1986, A&A, 157, L17
Guélin, M., Cernicharo, J., Paubert, G., & Turner, B. E. 1990, A&A, 230, L9
Guélin, M., Lucas, R., & Cernicharo, J. 1993, A&A, 280, L19
Guélin, M., Neininger, N., & Cernicharo, J. 1998, A&A, 335, L1
Guélin, M., Lucas, R., & Neri, R. 1997, in CO: Twenty-Five Years of Millimeter Wave Spectroscopy, ed. W. B. Latter et al. (Dordrecht: Kluwer), IAU Symp. 170, 359
Guélin, M., Muller, S., Cernicharo, J., et al. 2000, A&A, 363, L9
Guélin, M., Muller, S., Cernicharo, J., et al. 2004, A&A, 426, L49
Halfen, D. T., Clouthier, D. J., & Ziurys, L. M. 2008, ApJ, 677, L101
Kasai, Y., Obi, K., Ohshima, Y., et al. 1993, ApJ, 410, L45
Kawaguchi, K., Kagi, E., Hirano, T., et al. 1993, ApJ, 406, L39
Kawaguchi, K., Kasai, Y., Ishikawa, S.-I., & Kaifu, N. 1995, PASJ, 47, 853
MacKay, D. D. S. & Charnley, S. B. 2001, MNRAS, 325, 545
McCarthy, M. C., Gottlieb, C. A., Gupta, H., & Thaddeus, P. 2006, ApJ, 652, L141
Milam, S. N., Halfen, D. T., Tenenbaum, E. D., et al. 2008, ApJ, 684, 618
Millar, T. J., Flores, J. R., & Markwick, A. J. 2001, MNRAS, 327, 1173
Millar, T. J. 2008, Ap&SS, 313, 223
Ohishi, M., Kaifu, N., Kawaguchi, K., et al. 1989, ApJ, 435, L83
Pardo, J. R., Cernicharo, J., & Serabyn, E. 2001, IEEE Trans. Antennas Propag., 49, 1683
Pascoli, G. & Lavendy, H. 1998, Int. J. Mass Spectr., 181, 11
Pérez-Juste, I., Graña, A. M., Carballeira, L., & Mosquera, R. A. 2004, J. Chem. Phys., 121, 10447
Petrie, S. 1996, MNRAS, 282, 807
Petrie, S., Millar, T. J., & Markwick, A. J. 2003, MNRAS, 341, 609
Pham-Tran, N.-N., Hajgató, B., Veszprémi, T., & Nguyen, M. T. 2001, Phys. Chem. Chem. Phys., 3, 1588
Priem, D., Cosléou, J., Demaison, J., et al. 1998, J. Mol. Spec., 191, 183
Sims, I. R., Queffelec, J.-L., Travers, D., et al. 1993, Chem. Phys. Lett., 211, 461
Tenenbaum, E. D., Apponi, A. J., Ziurys, L. M., et al. 2006, ApJ, 649, L17
Tenenbaum, E. D. & Ziurys, L. M. 2008, ApJ, 680, L121
Woon, D. E. 1996, ApJ, 456, 602
Yang, D. L., Yu, T., Lin, M. C., & Melius, C. F. 1992, J. Chem. Phys., 97, 222
Ziurys, L. M., Apponi, A. J., Guélin, M., & Cernicharo, J. 1995, ApJ, 445, L47
Ziurys, L. M., Savage, C., Highberger, J. L., et al. 2002, ApJ, 564, L45

Appendix A: Spectra covering detected and non detected lines in the 3 mm band

In the case of silyl cyanide the three rotational transitions covered within the 3 mm band are observed, but for the molecules C_5S, MgCCH, and NCCP not all rotational transitions lying in the 3 mm band (80-116 GHz) are detected. The lines which are not detected either fall in spectral regions where the sensitivity achieved is not good enough or are blended with stronger lines of other molecules.

In Fig. A.1 we show the spectra covering the $J = 44 - 43$ to $J = 50 - 49$ rotational transitions of C_5S, lying in the low frequency side (80-93 GHz) of the 3 mm band. Only the three rotational transitions lying at the lowest frequencies ($J = 44-43$, $J = 45 - 44$, and $J = 46 - 45$) are detected (lines also shown in Fig. 1 and already discussed in section 3.1). The spectral regions where the next higher J lines of C_5S are expected are shown in the upper panels of Fig. A.1. None of these transitions can be identified with clear emission features in the observed spectra. The spectral region around the $J = 47 - 46$ and $J = 49 - 48$ transitions are relatively noisy. The antenna temperature rms noise level per 1 MHz channel is 1.5 mK around the $J = 47 - 46$ transition, while the expected C_5S line intensity is similar, making very difficult to ascertain whether or not the weak C_5S line is present. The situation is even worse for the $J = 49 - 48$ transition, with an expected antenna temperature of just ∼1 mK and a rms noise level of 1.8 mK per 1 MHz channel. The $J = 48 - 47$ and $J = 50 - 49$ transitions of C_5S are severely blended with other lines much stronger. At higher frequencies the chances of observing a C_5S line become lower because the expected C_5S line intensities decrease as J increases (C_5S is a quite heavy rotor and levels with $J > 50$ become poorly populated at rotational temperatures around 20 K) and also because in our 3 mm line survey of IRC +10216 spectra usually become less sensitive with increasing frequency.

As concerns the molecule MgCCH, there are three doublets of rotational transitions lying within the 3 mm band (see Fig. A.2). The two doublets lying at lower frequencies are identified with weak emission features (see also Fig. 2 and section 3.2) but the one lying at 109.2 GHz, corresponding to the $N = 11-10$ rotational transition, cannot be clearly distinguised in the 3 mm line survey data. The low frequency component of this doublet is completely blended with a stronger line arising from an hyperfine component of the $N_J = 1_2 - 0_1$ rotational transition of ^{13}CN, while the high frequency component cannot be appreciated due to an insufficient sensitivity (the T_A^* rms noise level is 1.8 mK per 1 MHz in this spectral region and the MgCCH component is expected with an intensity of just ∼1.5 mK).

The linear rotor NCCP has also several rotational transitions lying in the 80-116 GHz range (see Fig. A.3), from which only three ($J = 15 - 14$, $J = 16 - 15$, and $J = 18 - 17$) are identified with weak emission features (see also Fig. 3 and section 3.3). The $J = 17 - 16$ transition falls in a spectral region crowded by stronger lines arising from $CH^{13}CN$, and unidentified line at 91953 MHz, and CH_3CN, making very difficult to infer its presence. The $J = 19 - 18$ transition is partially blended with a stronger line corresponding to C_5N^-, and in any case the limited sensitivity of the spectrum (rms of 1.5 mK per 1 MHz) makes it very difficult to distinguish the NCCP line from the noise. An even worse situation occurs in the case of the $J = 20 - 19$ transition, which falls in a spectral region where it partially overlaps with a line of C_2P and the data is quite noisy (rms of 2.1 mK per 1 MHz). The last transition of NCCP within the 3 mm band is the $J = 21-20$, which falls in a spectral region where the noise level

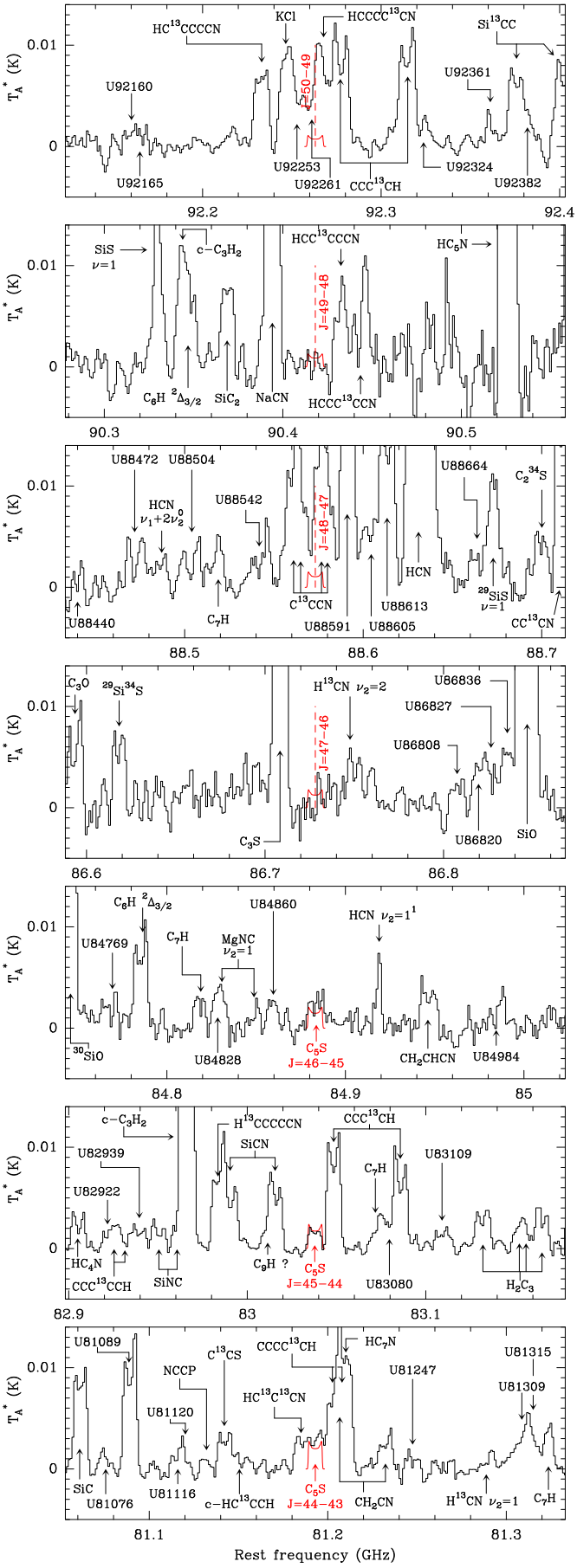

Fig. A.1. Spectra covering the C_5S lines in the 80-93 GHz frequency range. Detected lines are indicated by red arrows and non detected lines by red dashed lines. LTE calculated line profiles are shown in red.

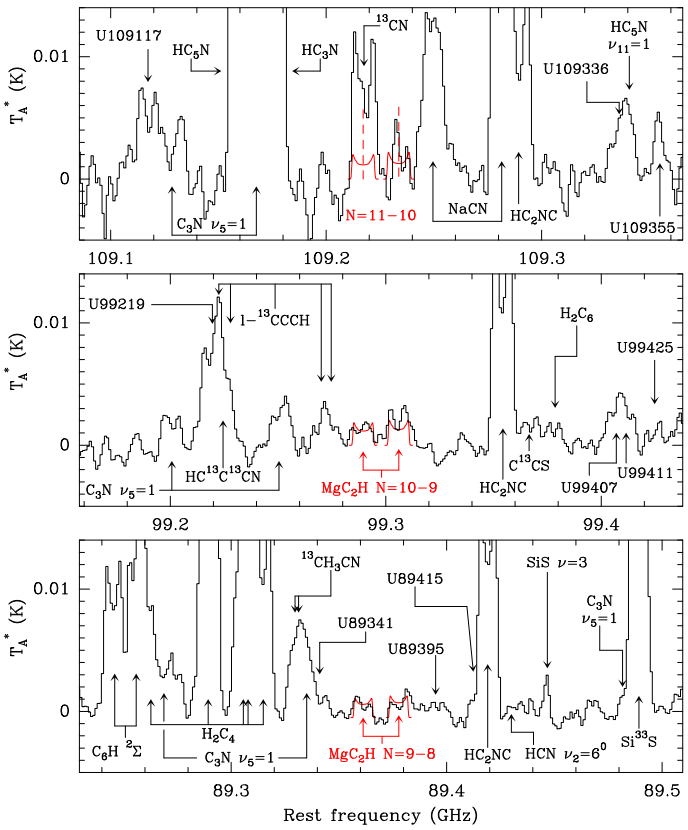

Fig. A.2. Spectra covering the MgCCH lines in the 3 mm band. Detected lines are indicated by red arrows and non detected lines by red dashed lines. LTE calculated line profiles are shown in red.

is moderately low (rms of 1.1 mK per 1 MHz if we do not consider the much noiser region at frequencies higher than 113600 MHz), although it is not low enough to allow for a clear detection of lines with antenna temperatures of ∼1 mK, as expected for this NCCP line.

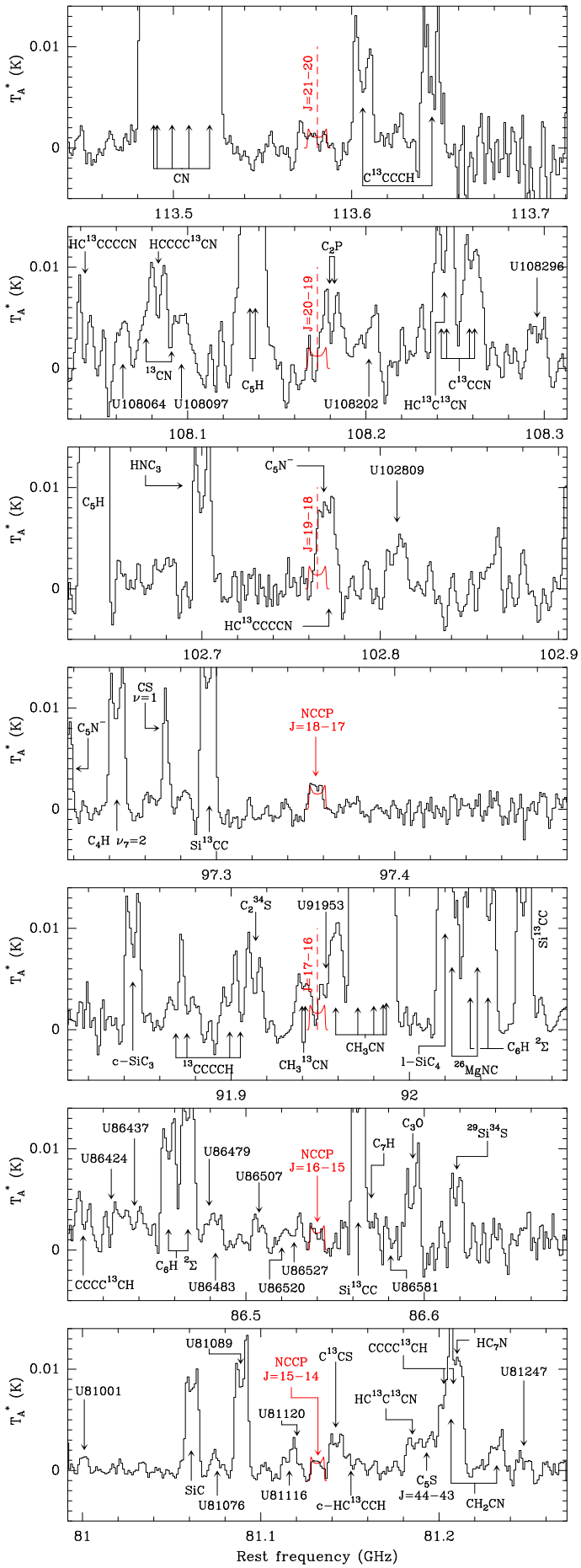

Fig. A.3. Spectra covering the NCCP lines in the 3 mm band. Detected lines are indicated by red arrows and non detected lines by red dashed lines. LTE calculated line profiles are shown in red.